

Thermal, ANFIS, and Polynomial Neural Network Models for Predicting Environmental Variables in an Arch Greenhouse

J. Javadi Moghaddam^{1*}, D. Momeni¹, and Gh. Zarei¹

ABSTRACT

The aim of this study was to design an Adaptive Neuro-Fuzzy Inference Mechanism (ANFIS) and a Polynomial Neural-Network (PNN) to improve modeling and identification of some climate variables within a greenhouse. Furthermore, a Stable Deviation Quantum-Behaved Particle Swarm Optimization (SD-QPSO) algorithm was employed as a learning algorithm to train the constant parameters of ANFIS and PNN structures. To denoise measured data, a wavelet transform method was applied to ensure that no measured data exceeds a predefined interval. Moreover, to show the modeling performance, a set of differential equations were derived as a dynamical model based on the computation of energy and mass balance in a specified greenhouse. The results of modeling and simulation were evaluated with the experimental results of an experimental arch greenhouse. The results showed that the proposed models were more accurate in predicting greenhouse climate and could be used more easily. Moreover, this study showed that the PNN model with less pop-size and evaluation function was more effective than the ANFIS structure to predict the temperatures of inside air and inside roof cover. In this study, an on-line identification system is also proposed for real time identification of experimental data. The obtained simulation results show that performance of the proposed modeling structures and identification system are effective to predict and identify the soil surface, internal air, and roof cover temperatures of the greenhouse. This study shows that the identification algorithm can be used to predict and confirm the results of the model.

Keywords: Denoising data, Modeling, PNN, SD-QPSO, Wavelet.

INTRODUCTION

The greenhouse is considered as an uncertain and a very complex dynamic nonlinear system that is covered with thin and transparent materials. The disturbance variables such as external air temperature, radiation, wind speed and humidity increase the nonlinearity property of greenhouses. Therefore, difficulties to improve the accuracy in the greenhouse controller design such as climate control systems and the optimization methods to save the energy demand are increased. To develop the greenhouse automation, Grigoriu *et al.* (2015) provided heat for a specified greenhouse by use of parabolic trough collector thermal energy and designed a control system to regulate the internal temperature of the greenhouse. They induced a

proper signal as an input to climate control system of a greenhouse. However, to design precise control systems, a clear physical explanation of the greenhouse environment can be helpful. Hence, many modeling strategies and optimization methods have been proposed for greenhouse simulation and control over the years. To design a practical control system based on a fairly accurate model for greenhouse temperature, Márquez-Vera *et al.* (2016) presented a fuzzy model of the internal temperature of a greenhouse and developed a fuzzy controller to adjust the internal temperature. Moreover, Isaev and Sadykov (2014) presented a mathematical model of the heat exchange process based on analytical approach in a solar greenhouse. Su and Xu (2017) presented a discrete-time greenhouse

¹ Agricultural Engineering Research Institute (AERI), Agricultural Research Education and Extension Organization (AREEO), Karaj, Islamic Republic of Iran.

* Corresponding author; e-mail: jalaljavadmoghaddam@gmail.com



climate model and designed a greenhouse climate discrete control based on an algebraic fitting technique and time sequence functions. They employed a polynomial to estimate and identify unknown parameters and some unmodeled dynamics based on the least square and Levenberg-Marquardt (LM) algorithms. Fidaros *et al.* (2010) developed a numerical simulation based on finite volume to investigate the uniform transfer of air due to ventilation that occurs inside an arch type of tunnel greenhouse during a solar day. As can be seen, many models have been proposed to improve the climate control systems to save the energy demand. Therefore, preparing a precise greenhouse climate model becomes a challenge in engineering studies. Hence, Sethi *et al.* (2013) compared the performance of some climate thermal models and heating methods in the analysis of greenhouses. To achieve a realistic simulation of greenhouse climate modeling, steady state conditions of the glazing cover inside, air, and soil should be considered. The steady state analysis can be used to calculate the total additional energy required in a greenhouse (Mobtaker *et al.*, 2016). Thus, Joudi and Farhan (2007) proposed a dynamic model to predict the inside air and soil temperature of a greenhouse with less than 10% absolute error. Many artificial intelligence modeling techniques, such as the artificial neural network (Fourati and Chtourou, 2007; González and Calderón, 2018; García *et al.*, 2020; He and Ma, 2010) have been developed for modeling and controlling the climate of the greenhouse based on roof cover, soil temperature, and air temperature.

For greenhouse climate control modeling, the sampling time to collect the data is important. It should be noted that the run time of calculations increases with a lot of collected data. However, a small data set may provide inaccurate model for the control purposes. Therefore, Speetjens *et al.* (2009) developed an adaptive extended Kalman filter for on-line estimation of climate parameters in a greenhouse model with data collected over a year. Numerous non-linear control laws have been used to control climate in greenhouses such as system linearization (Pasgianos *et al.*, 2003) and adaptive fuzzy control (Su *et al.*, 2016). The main objective of the climate control design is to set the humidity and the temperature of the greenhouse environment in the vicinity of a

predefined and desired values. Moreover, in many studies, the metaheuristic optimization algorithms such as PSO, Quantum-Behaved Particle Swarm Optimization (QPSO) have been applied to solve the optimization problems and to find the constant parameters of a specified model. Yu *et al.* (2016) presented a temperature prediction model based on a least squares support vector machine and applied a PSO algorithm with probability of mutation to optimized parameters in a model. Chen *et al.* (2016) proposed a model optimized prediction methodology to predict the energy demand of greenhouses with a better performance of accuracy and reduction in runtime or computation time. They employed an adaptive particle swarm optimization to calibrate the uncertain parameters by using experimental data.

Perez-Gonzalez *et al.* (2017) presented a collection method based on Particle Swarm Optimization (PSO) and Differential Evolution (DE) to identify the parameters of a mathematical model for a greenhouse. Hu *et al.* (2014) proposed a methodology based on nondominated sorting genetic algorithm- II (NSGA-II) for tuning the parameters for multiple PID controllers to climate control of a greenhouse.

The sensitivity analysis can be done to show the sensitivity of a model on input data. Kurtulus *et al.* (2010) proposed an ANFIS model with two triangular MF per node to assess the resulting hydraulic head distribution. They added a systematic error of -2 m, -1 m, 1 m, and 2 m to the soil elevation of each cell and then compared the results of ANFIS output due to this error than the output reference and, thus, this difference showed the model sensitivity.

Based on the static energy balance of the greenhouse components, Ziapour and Dehnavi (2012) proposed a finite-volume method for solving the energy balance in the arc-roof and one-sided roof enclosures for greenhouse boundary conditions. Using multiple linear regressions, Rosas *et al.* (2017) developed a semi-empirical dynamic model of energy balance to predict temperatures of a naturally ventilated greenhouse in a Mediterranean climate, where the solar radiation was the main component of the energy balance in warm climate conditions.

The problem of temperature estimation in a greenhouse system has been paid a lot of attention and thus many observation and identification systems, such as Ferreira *et al.* (2002) and Patila *et al.* (2008), have been developed in recent years. The neural networks can be used for system identification effectively. However, the time delay due to online learning by the adaptive rules is a problem, indeed. Therefore, sliding mode observer can be used as a fast response observer with a robustness property and high-performance operation. Hence, Fridman *et al.* (2007) proposed a higher-order sliding-mode observer for linear time invariant systems. The single output and unknown bounded single input are some specifications in this observer. Therefore, the results of sliding-mode observer such as this method can be extended to the multi-input multi-output (MIMO) cases and thus many authors have developed the higher order sliding mode observers for the MIMO nonlinear systems (Floquet *et al.*, 2007).

Although various methods have been proposed for modeling and predicting greenhouse climates, it is not yet clear how reliable their results are. Changes in boundary conditions outside the greenhouse, as well as changes in evapotranspiration rates, cause changes in data collection conditions. Therefore, the error can increase due to the response of mathematical models. As a result, the greenhouse climate-control-systems that use these models cannot be practical and appropriate. Therefore, in this study, a method for modeling and predicting greenhouse climate was presented that can be used industrially and practically.

In the next section, specification of constructed arch greenhouse and a dynamic model derived based on mass and energy balance are presented. Moreover, the proposed ANFIS and PNN models with their optimization algorithm are explained and the results of the proposed models are compared with the experimental data by some simulations.

MATERIALS AND METHODS

Dynamic Model

In this section, three differential equations were derived to simulate the inside air, roof cover, and the soil surface temperatures. This dynamical model was derived from the energy balance equation for the inside air, the roof area, and the topsoil (Van-Straten *et al.*, 2011). It was assumed that the greenhouse elements were considered as lumped systems and evaporation did not occur from the soil surface. Furthermore, no absorption and emission of the radiation energy occurred by the inside air. The uniform temperatures of topsoil layer and air were assumed in computation and the constructed greenhouse had no plants during the recording data. To drive the energy balance equations, the heat transfer coefficients between the surfaces in the greenhouse can be written as follows (Van-Ooteghem, 2007):

$$\alpha_{a,s} = 1.7|T_{air} - T_{soil}|^{\frac{1}{3}} \quad \forall T_{air} < T_{soil} \quad (1)$$

$$\alpha_{a,s} = 1.3|T_{air} - T_{soil}|^{\frac{1}{4}} \quad \forall T_{air} \geq T_{soil} \quad (2)$$

$$\alpha_{ri,o} = 2.8 + 1.2 V_{out} \quad \forall V_{out} < 4 \quad (3)$$

$$\alpha_{ri,o} = 2.5 V_{out}^{0.8} \quad \forall V_{out} \geq 4 \quad (4)$$

A combination of the energy balance and the transferred energy of the greenhouse between the elements (De-Zwart, 1996) and with estimated infiltration through the greenhouse (Vadiee, 2011) can be expressed by the following forms:

$$\frac{dT_{soil}}{dt} = \frac{1}{\rho_s c_{ps} V_s} (Q_{rds} + A_{soil} \alpha_{a,s} (T_{air}(t) - T_{soil}(t)) - Q_{sri}) - \frac{A_{soil} \lambda_s (T_{soil}(t) - T_{ss}(t))}{\rho_s c_{ps} V_s ds} \quad (5)$$

$$\frac{dT_{roof}}{dt} = \frac{1}{\rho_r c_{pr} V_r} (Q_{rdri} + 3A_{roof} |T_{air}(t) - T_{roof}(t)|^{1/3} (T_{air}(t) - T_{roof}(t)) + Q_{sri} - A_{roof} \alpha_{rio} (T_{roof}(t) - T_{out}(t)) - Q_{risk}) \quad (6)$$

$$\frac{dT_{air}}{dt} = \frac{1}{\rho_a c_{pa} V_a} (A_{soil} \alpha_{a,s} (T_{air}(t) - T_{soil}(t)) - \rho_a c_{pa} A_{soil} (8.3 \times 10^{-5} + 3.5 \times 10^{-5} V_{out} f_a) (T_{air}(t) - T_{out}(t)) - 3A_{roof} |T_{air}(t) - T_{roof}(t)|^{1/3} (T_{air}(t) - T_{roof}(t)) - \frac{A_{nw} \lambda_{nw} (T_{nw}(t) - T_{nwi}(t))}{d_{nw}}) \quad (7)$$

where, Q_{rds} and Q_{rdri} are the solar radiation absorbed by the soil surface and roof, respectively, and their computational equations



can be considered as Van-Ooteghem (2007). By substituting the values of Q_{rds} , Q_{rdri} , the net solar radiation heat exchange between soil and roof Q_{sri} , and the net solar radiation heat exchange between roof and sky Q_{risk} (Van-Straten et al., 2011) in the above equations, one can obtain Equation (8):

$$\frac{dT_{soil}}{dt} = \frac{1}{\rho_s c_{ps} V_s} \left(A_{soil} \eta_{sis} I_{in} + A_{soil} \alpha_{a,s} (T_{air}(t) - T_s(t)) - A_{soil} E_s E_{ri} F_{sri} \sigma (T_{soil}^4 - T_{roof}^4) \right) - \frac{A_{soil} \lambda_s (T_s(t) - T_{ss}(t))}{\rho_s c_{ps} V_s ds} \quad (8)$$

$$\frac{dT_{roof}}{dt} = \frac{1}{\rho_r c_{pr} V_r} \left(A_{roof} \eta_{roofls} I_{roof} + 3A_{roof} |T_{air}(t) - T_{roof}(t)|^{1/3} (T_{air}(t) - T_{roof}(t)) + A_{soil} E_s E_{ri} F_{sri} \sigma (T_{soil}^4 - T_{roof}^4) - A_{roof} \alpha_{ri,o} (T_{roof}(t) - T_{out}(t)) - A_{roof} E_{ri} E_{sk} F_{risk} \sigma (T_{roof}^4 - T_{sky}^4) \right) \quad (9)$$

$$\frac{dT_{air}}{dt} = \frac{1}{\rho_a c_{pa} V_a} \left(A_{soil} \alpha_{as} (T_{air}(t) - T_{soil}(t)) - \rho_a c_{pa} A_{soil} (8.3 \times 10^{-5} + 3.5 \times 10^{-5} V_{out} f_a) (T_{air}(t) - T_{out}(t)) - 3A_{roof} |T_{air}(t) - T_{roof}(t)|^{1/3} (T_{air}(t) - T_{roof}(t)) - \frac{A_{nw} \lambda_{nw} (T_{nw}(t) - T_{nwi}(t))}{d_{nw}} \right) \quad (10)$$

Some literature propose a method to find the sky temperature. In this study, the sky temperature is presented as $T_{sky}(t) = 0.0552(T_{out}(t))^{1.5}$ (Joudi and Farhan, 2007). Therefore, Equation (9) can be rewritten as the following expression:

$$\frac{dT_{roof}}{dt} = \frac{1}{\rho_r c_{pr} V_r} \left\{ A_{roof} \eta_{roofls} I_{roof} + 3A_{roof} |T_{air}(t) - T_{roof}(t)|^{1/3} (T_{air}(t) - T_{roof}(t)) + A_{soil} E_s E_{ri} F_{sri} \sigma (T_{soil}^4 - T_{roof}^4) - A_{roof} \alpha_{ri,o} (T_{roof}(t) - T_{out}(t)) - A_{roof} E_{ri} E_{sk} F_{risk} \sigma [T_{roof}^4 - (0.0552(T_{out}(t))^{1.5})^4] \right\} \quad (11)$$

Where, $\sigma = 5.67051 \times 10^{-8} W/m^2 K^4$ is Stefan-Boltzman constant.

Equations (8), (10), and (11) were solved at each time step using appropriate values of input parameters. In the dynamic equations, T_{soil} , T_{air} , and T_{roof} were state variables, and the variables T_{out} , V_{out} , I_{in} , and I_{roof} were considered as

input or boundary variables. It should be noted that some parameters and coefficients of the dynamic equation of the greenhouse must be calculated according to the experimental conditions to improve the result in practice. Otherwise, these equations will have a significant error. On the other hand, measuring these parameters, such as thermal coefficients that change over time, can be difficult. Therefore, the use of artificial intelligence algorithms that directly and indirectly use the information of common sensors in the greenhouse, such as temperature, humidity, etc., can be more accurate in predicting the results of greenhouse climate behavior. Hence, an appropriate method for this issue was suggested in the following section.

SD-QPSO Algorithm and ANFIS Training

The SD-QPSO (Moghaddam and Bagheri, 2015) is a metaheuristic optimization algorithm that is based on the Quantum Behaved Particle Swarm Optimization (QPSO) algorithm. In this section, the SD-QPSO algorithm is applied to optimize the ANFIS parameters (Jang, 1993) in the rules layer and the least square method is also employed to find the Takagi-Sugeno coefficients. The main idea of the SD-QPSO is based on the QPSO algorithm, in which a stable deviation function is considered to improve the domain search. For the N number of particles, swarm set can be defined as $set = \{x_1, x_2, \dots, x_N\}$. The position and the velocity i^{th} of particles can be considered as $x_i = (x_{i1}, x_{i2}, \dots, x_{iD})^T$ and $v_i = (v_{i1}, v_{i2}, \dots, v_{in})^T$ for $i = 1, 2, \dots, N$, respectively. In this algorithm, the best positions $p_i = (p_{i1}, p_{i2}, \dots, p_{in})^T$ for a history set $P = \{P_1, P_2, \dots, P_N\}$ can be defined in which $p = argmin_t f_i(.)$ for $i = 1, 2, \dots, N$. Here, t is an iteration counter and $f_i(.)$ is the objective function. In this study, the position and the velocity can be written as x_{ij}^t and v_{ij}^t , respectively. The basic iterative equations of the QPSO can be considered by the following forms:

$$x_{ij}^{t+1} = P_{ij}^t + \beta |mbest - x_{ij}^t| \ln\left(\frac{1}{u}\right) \text{ if } k \geq 0.5 \quad (12)$$

$$x_{ij}^{t+1} = P_{ij}^t - \beta |mbest - x_{ij}^t| \ln\left(\frac{1}{u}\right) \text{ if } k < 0.5 \quad (13)$$

Where, β is called contraction–expansion coefficient and u is a random number.

$$P_{ij}^t = \frac{c_1 P_{ij}^t + c_2 P_{gj}^t}{c_1 + c_2} \quad (14)$$

The random numbers c_1 and c_2 are selected uniformly from the interval $[0, 1]$. The mean best (mbest) of population is defined as the mean of the best positions of all particles and can be obtained as:

$$mbest = \frac{1}{M} \sum_{i=1}^M P_i \quad (15)$$

The history set can be also substituted by the best position and, therefore, the mbest can be expressed as:

$$mbest = \left(\frac{1}{M} \sum_{i=1}^M P_{i1}, \frac{1}{M} \sum_{i=1}^M P_{i2}, \dots, \frac{1}{M} \sum_{i=1}^M P_{ij} \right) \quad (16)$$

In the SD-QPSO algorithm, a swarm can be generated by a nonlinear function. The evaluation of new swarm shows that it can be accepted and replaced in position of the worst particle in the swarm. This way is applied, while no better solution is obtained, then, a particle that is selected as $a = X_{min}$ with two randomly chosen swarm particles $\{b, c\}$ from the population are used to generate a new particle with a fair fitness. So, a crossover operator is used to generate this solution vector at the minimum point of the quadratic curve passing through three different selected swarm particles $\{a, b, c\}$. Therefore, this method can improve diversity and probability to find a better particle in the search space. In this method, a recombination operator is defined to generate the first candidate particle x_{pz}^t as follows:

$$x_{pz}^t = \frac{1}{2} \frac{(b_z^2 - c_z^2)f(a_z) + (c_z^2 - a_z^2)f(b_z) + (a_z^2 - b_z^2)f(c_z)}{(b_z - c_z)f(a_z) + (c_z - a_z)f(b_z) + (a_z - b_z)f(c_z)} \quad (17)$$

The stable deviation function as a parallel recombination operator is defined to generate the second candidate particle x_{qz}^t by the following form:

$$x_{qz}^t = \frac{(b_z - c_z)^2 f^2(a_z)}{(b_z - c_z)^2 f^2(a_z) + 1} \tanh((b_z - c_z)f(a_z)) + \frac{(c_z - a_z)^2 f^2(b_z)}{(c_z - a_z)^2 f^2(b_z) + 1} \tanh((c_z - a_z)f(b_z)) + \frac{(a_z - b_z)^2 f^2(c_z)}{(a_z - b_z)^2 f^2(c_z) + 1} \tanh((a_z - b_z)f(c_z)) \quad (18)$$

The sum of absolute errors was considered as an objective function. Finally, the global best position of the particles is considered as the optimized parameters in the rule layer. To

develop the modeling, evaluation results, and sensitivity analysis, a PNN structure was also considered for the comparison purposes. The structure of the proposed PNN model, which was optimized by the SD-QPSO algorithm, is presented in the following section.

Polynomial Neural Network (PNN)

To show the model sensitivity analysis and model evaluation, a PNN was proposed and the SD-QPSO algorithm was utilized to obtain the constant parameters and coefficients. The main function of PNN can be written as:

$$F_0(\alpha_i, x_{z,j}) = \sum_{i=1}^3 \pi_i(\alpha_i, x_{z,j}) \quad (19)$$

Where, the linear and the nonlinear parts of function (19) are considered by the following forms:

$$\pi_1(\alpha_i, x_{z,j}) = \sum_{i,j=1}^{m_1} F_i(\alpha_i, x_{z,j}) = \sum_{i,j=1}^{m_1} \alpha_i x_{z,j} \quad (20)$$

$$\pi_2(\alpha_i, x_{z,j}) = \sum_{i=1}^{m_2} \sum_{j=i+1}^{m_3} \alpha_n F_i F_j, \quad (21)$$

$$\pi_3(\alpha_i, x_{z,j}) = \sum_{i=1}^{m_4} \sum_{i \neq j, j=1}^{m_5} \alpha_n F_i^2 F_j, \quad (22)$$

Where, n is an appropriate increased counter and m_1, m_2, \dots, m_5 are selected to be equal to the number of input variables. The Mean Absolute Error (MAE) between the observed and the experimental data are considered as the cost function that is presented by the following form:

$$MAE = [\sum_{i=1}^n |exdata_i - obdata_i| / N] \quad (23)$$

The learning methodology to train the proposed PNN model is developed by the following algorithm:

Choose the number of inputs and constant parameters based on the polynomial degree of PNN.

Choose 70% of data as the training procedure.

Random initialize the constant parameters of PNN model.

Set the evaluation and pop size number of SD-QPSO algorithm in which the MAE results between output model and experimental data satisfy a predefined threshold.

Use the SD-QPSO algorithm to find constant parameters of PNN model.

Use the optimized constant parameters from the last step in the PNN model and check the train and the test quality.



In modeling, it should be noted that data are collected and categorized at predetermined sample times. Therefore, any power failure or sensor failure that prevents the data from being recorded correctly can increase the modeling error. Mathematical identification algorithms can be used to ensure the accuracy of the measured variables. In addition, some of the necessary parameters in predicting the dynamic behavior of the greenhouse can be identified online using these mathematical methods. In this research, the robust identification method used to examine temperature data is presented in the following section.

System Identification of Greenhouse

To investigate the rate of heat transfer and to improve the energy consumption in a greenhouse, an identification method can be useful for on-line estimation of temperature changes in a greenhouse. However, many different identification systems have been developed recently; the use of sliding mode in hi-tech greenhouses has interested many authors (Yau and Chen, 2011) because of its fast converging and easy implementation. To design a sliding mode identification system, the chattering phenomena can be considered as a major problem. Therefore, in this section, a system identification method based on the higher order sliding mode identification (Levant, 1993) is proposed to smoothly identify the average of daily temperature variables of soil surface, internal air, and roof cover of the constructed greenhouse. The proposed simple identification algorithm is presented by the following equations:

$$\begin{aligned}\dot{\hat{x}}_1 &= \tilde{x}_2 + \lambda_1 |e_1|^{1/2} \frac{e_1^2}{(\delta_1 + e_1^2)} \tanh(e_1) \\ \dot{\hat{x}}_2 &= \alpha_1 \frac{e_1^2}{(\delta_1 + e_1^2)} \tanh(e_1) \\ \dot{\hat{x}}_2 &= E_1 \left[\tilde{x}_3 + \lambda_2 |e_2|^{1/2} \frac{e_2^2}{(\delta_2 + e_2^2)} \tanh(e_2) \right] \\ \dot{\hat{x}}_3 &= E_1 \alpha_2 \frac{e_2^2}{(\delta_2 + e_2^2)} \tanh(e_2) \\ \dot{\hat{x}}_3 &= E_2 \left[\tilde{x}_4 + \lambda_3 |e_3|^{1/2} \frac{e_3^2}{(\delta_3 + e_3^2)} \tanh(e_3) \right] \\ \dot{\hat{x}}_{n-1} &= E_{n-3} \alpha_{n-2} \frac{e_{n-2}^2}{(\delta_{n-2} + e_{n-2}^2)} \tanh(e_{n-2})\end{aligned}$$

$$\begin{aligned}\dot{\hat{x}}_{n-1} &= \\ E_{n-2} &\left[\tilde{x}_n + \right. \\ \lambda_{n-1} |e_{n-1}|^{1/2} &\frac{e_{n-1}^2}{(\delta_{n-1} + e_{n-1}^2)} \tanh(e_{n-1}) \left. \right] \\ \dot{\hat{x}}_n &= E_{n-2} \alpha_{n-1} \frac{e_{n-1}^2}{(\delta_{n-1} + e_{n-1}^2)} \tanh(e_{n-1}) \\ \dot{\hat{x}}_n &= E_{n-1} \left[\tilde{\theta} + \lambda_n |e_n|^{1/2} \frac{e_n^2}{(\delta_n + e_n^2)} \tanh(e_n) \right] \\ \dot{\hat{\theta}} &= E_{n-1} \alpha_n \frac{e_n^2}{(\delta_n + e_n^2)} \tanh(e_n)\end{aligned}\quad (24)$$

Where, $e_i = \tilde{x}_i - \hat{x}_i$ is the error term between experimental (\tilde{x}) and estimated data (\hat{x}) for $i = 1, \dots, n$ with $\tilde{x}_1 = x_1$ and $[\tilde{x}_i, \tilde{\theta}]$ is the output of the proposed observer. There is a constant parameter $\delta_i \in [1, 1.5]$ to have a smooth response. $|\alpha(t)| \leq K$ is a bounded smooth scalar function and K is a positive constant. In Equation (24), the sign function in the original sliding mode identification (Levant, 1993) has been replaced by $\frac{e_i^2}{(\delta_i + e_i^2)} \tanh(e_i)$ to induce more smooth response. The scalar functions E_i are defined as

$$E_i = 1 \text{ if } |e_j| = |\tilde{x}_j - \hat{x}_j| \leq \varepsilon, \text{ for all } j \leq i \text{ else } E_i = 0 \quad (25)$$

Where, ε is a small positive constant.

In the following, the experimental conditions and the result of using the mentioned modeling and identification functions are described.

RESULTS AND DISCUSSION

Structure of Greenhouse and Data Recording

In this study, the experimental data was collected in an arch greenhouse that was designed and constructed at the Southeast of Iran, in Kerman Province, city of Jiroft, with geographical coordinates of 57° 51' E and 28° 32' N, at an altitude of 750 m above the sea level. The structure of the constructed greenhouse is shown in Figure 1, with the base dimension of 5.5×40 m. It had a height of 3.5 m and designed according to receive maximum solar radiation. This experimental greenhouse was equipped with natural ventilation system, etc. The heating system with hot water was off during the data gathering. Therefore, due to the ability of loggers and its available space to store information, 6



Figure 1. Outside and inside views of the constructed greenhouse.

data were collected daily for the following variables every one hour (between 10:00 to 17:00) and the average (to reduce the sensitivity of the model) was used as daily data (Dates of data recording and measurement: 22/11/2007 to 05/04/2008.): T_{air} , T_{roof} , T_{out} , I_{roof} , V_{out} , T_{soil} , RH_{air} and RH_{out} . Then, it was applied as a new sampling time in modelling. To do this, four CEM DT-171T sensors were used to

measure the temperature of the inside air, soil, and roof cover as well as relative humidity inside/outside the greenhouse. The constructed greenhouse was partitioned by sensors located on the soil, air (middle part of the greenhouse), inside the roof, and outside the greenhouse. Figure 2 shows the greenhouse dimensions and the sensor locations of the data logger system. It should be noted that the critical area of temperature in the greenhouse was located between the soil and indoor air sensors, which could be used to determine the optimal conditions for plant growth. In the next section, to demonstrate the efficiency of the dynamic equations, the results are compared with the data collected by the greenhouse sensors. Simulations in this study were performed using MATLAB software version 2016A. Moreover, ANFIS and PNN models as well as identification and SD-QPSO algorithms were programmed in this software.

Dynamic Results

In this section, the results of differential Equations (8), (10) and (11) are compared with the experimental data. All initial conditions were based on experimental data at the beginning of the operation. The conditions considered for input variables were as follows: $T_{out} = 16$, $V_{out} = 8.48$, $I_{in} = 10.85$, and $I_{roof} = 6.2$. The initial values for the state variables were $T_{soil} = 15.5^{\circ}\text{C}$, $T_{air} = 17^{\circ}\text{C}$, and $T_{roof} = 17^{\circ}\text{C}$. Moreover, other nominal parameters of greenhouse dynamic equations were considered according to Table 1.

Table 1. Parameters used in calculations.

Parameter	Value	Parameter	Value	Parameter	Value
ρ_s	1400	c_{pa}	1000	ds	0.8
c_{ps}	800	E_s	0.7	ρ_r	2500
V_s	352	E_{ri}	0.95	η_{roofIs}	0.0173
A_{soil}	440	F_{sri}	0.8	ρ_a	1.21
η_{sIs}	0.86	T_{ss}	4	c_{pr}	840
A_{roof}	314	V_r	0.9420	λ_s	0.6
T_{nwo}	$T_{out} - 0.5T_{air}$	V_a	1382.5	d_{nw}	0.25
T_{nwi}	$T_{air} - 0.9T_{out}$	λ_{nw}	0.397	f_a	1
A_{nw}	34.5625				

To solve the differential equations of the system, two MATLAB Files (m.file: MATLAB programming environment) were programmed in MATLAB environment. The program of the first m.file included the function of greenhouse dynamic equations, constants, variables and how to receive and send input and output variables. The second file program included the method of solving the differential equation of the first m.file, reading experimental data for comparison from an Excel file, and instructions for drawing 2D and 3D graphs. To solve the differential equations, the ode45 Toolbox was used with automatic accuracy. The statistical results of the dynamic greenhouse model for T_{soil} were presented as follows: $MAPE = 2.2733$, $EF = 0.9357$, $TSSE = 0.2995$, $RMSE = 0.5873$ and $R^2 = 0.9550$. Moreover, the results of statistical calculations using dynamic model for prediction of $T_{air} = 17^\circ\text{C}$, and $T_{roof} = 17^\circ\text{C}$ are in Tables 2 and 3. Figures 3a) and 3b) show the results of the dynamic model and the comparison of the error response of the experimental data over a period of 134 days. In the use of dynamical method, researchers have accepted the error less than 20% (Joudi and Farhan, 2007). It should be noted that, because of the materials properties and some assumptions to derive the equations, comparison between the measured data and dynamical response are not recommended. Therefore, it can be shown as differences between nominal and real conditions during the work. These differences can be sorted as T_{soil} , T_{air} and T_{roof} . The small error response before day 90th shows that in cold weather the results of

dynamical model were close to the experimental data. Closing the opening in winter was the main reason, because it reduced the effect of disturbances caused by outside wind speeds. In this study, we tried to select the constant coefficients of dynamic equations in such a way to have the highest correlation between the results of dynamic equations of the greenhouse and experimental data. Figure 3 shows that the maximum and minimum differences are between the roof temperature and the soil temperature, respectively. The reason can be attributed to the effect of wind speed outside the greenhouse and the intensity of radiation on the roof of the greenhouse. In addition, the temperature close to the greenhouse cover was strongly influenced by the climate outside the greenhouse. On the other hand, due to sunlight on the soil surface and increasing heat, the air movement will always be in the direction perpendicular to the soil and, as a result, the temperature steady state changes in the experiment. In this case, we cannot expect the results of dynamic equations to be very accurate without calibrating their coefficients. The following shows how the use of predictive numerical algorithms can increase the accuracy of predicting greenhouse climate behavior.

Results of ANFIS and PNN Modeling by SD-QPSO

The average of one day was considered as an experimental data to reduce the computation and, thus, 134 experimental data was gathered for each variable parameters of T_{air} , T_{roof} , T_{out} ,

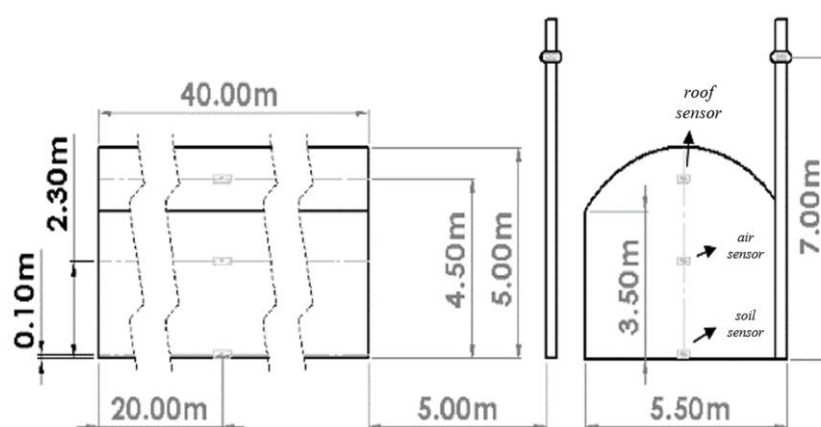


Figure 2. The greenhouse dimensions and the sensor locations.

I_{roof} , V_{out} , T_{soil} , RH_{air} and RH_{out} . Two different ANFIS and PNN structure were obtained to predict the T_{air} and T_{roof} due to the inputs of T_{soil} , T_{out} , I_{roof} , V_{out} , RH_{air} and RH_{out} . It is noted that the relation between T_{soil} with T_{air} and T_{roof} can improve the results of modeling (Taki *et al.*, 2016) and, therefore, the values of T_{soil} were considered as an input.

In the ANFIS mechanism, the three bell membership functions were considered for each input layer and ANFIS and PNN constant parameters were found by the SD-QPSO algorithm. Thirty-five constant parameters were used in PNN system and the numbers of population size and evaluation functions to train the ANFIS and PNN structure were set as [175, 210] and [112, 196], respectively. In order to equalize the effect of data type on computations, in many artificial intelligence systems and machine learning algorithms, the data should be normalized in the range [0, 1]. In the modeling procedure, a wavelet transformed was employed to denoise all data (To *et al.*, 2009).

Three m.files were programmed for ANFIS model. The first m.file was for starting and running the program. At first, the data was read from an Excel file. The wavelet transform toolbox was then used to denoise measured data. After normalization, the data were entered into the SD-QPSO algorithm. In each evaluation, the ANFIS program written in the second m.file was called by the mentioned optimization algorithm. After optimizing the coefficients of the ANFIS function based on the training data, the test data in the optimized function were used to show the performance of ANFIS model in the prediction. After that, the statistical results whose calculation program was written in the third m.file were called and printed. Finally, the program for creating custom graphs was implemented. The number of m.files and programming steps of the PNN model were the same as for ANFIS. The difference was that, in the second file, the PNN function program was written and all the coefficients and programming in the related files were changed according to the number of coefficients of this function.

The results of ANFIS model are depicted in Figure 4, from which the train and test data set were selected as 70% and 30%, respectively. Figure 4b shows a small error between trained

model output and experimental data, which increased in the test region. Figure 4a shows that this small error has a negligible effect on ANFIS model response. Here, the train and the test region were separated by a dashed line. The efficiency values such as the Mean Absolute Percentage Error (MAPE), Modelling Efficiency (EF), average (TSSE), coefficient of determination (R^2) and the Root Mean Squared Error (RMSE) due to ANFIS, PNN, and dynamic models are shown in Tables 2 and 3 for T_{air} and T_{roof} , respectively. The high accuracy and model performance of the ANFIS and PNN structure can be shown by the values of R^2 and RMSE. It has a value less than 0.99 and 0.28 in ANFIS and PNN modeling, respectively. Table 3 shows that, by using this structure to model T_{roof} , the maximum RMSE value decreased to less than 0.99. PNN model was more effective than ANFIS and dynamic models because of small values for RMSE, TSSE, MAPE, large values for R^2 and EF. The PNN model results and error response are depicted in Figures 5a and 5b, respectively.

In this study, the sensitivity analysis was performed to sort the effectiveness inputs in two different strategies. In the first strategy, based on the optimized PNN parameters, which were founded by the SD-QPSO algorithm, a +0.1 and a -0.1 deviation were added to each normalized input, while the others were fixed. The results can be obtained in Figures 6 and 7. Figures 6a and 7a show that T_{out} and RH_{out} are the most and least important inputs to model the T_{air} , respectively. It shows that changing of the outside temperature of greenhouse should be considered to design a temperature control system and the required power. Moreover, the relation between T_{soil} and T_{roof} are shown in Figures 6b and 7b. Solar radiation from the soil to the roof and the effect of RH_{air} on this reflection can be considered as the main reason in the results of sensitivity analysis. Because sunlight is refracted or absorbed by water droplets suspended in the air. In the second strategy, an input was removed and the effect of removed input on the output was investigated. The results shown in Figure 8 confirm the first strategy.

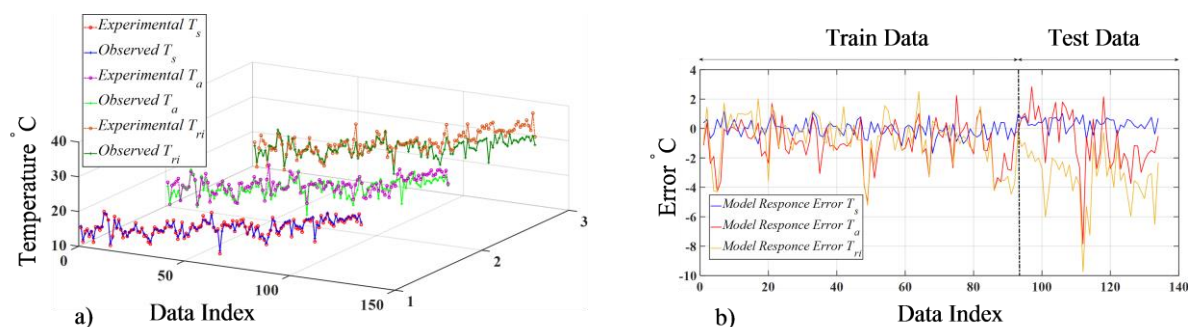
As mentioned, various assumptions should be considered to obtain the equations and the dynamic model of the greenhouse. These

**Table 2.** Efficiency values of T_{air} model.

Modelling structure	ANFIS		Polynomial		Dynamic Model	Identification system
	Train data	Test data	Train data	Test data		
MAPE	6.8381	5.0798	1.4925	1.2199		
EF	0.8068	0.9718	0.9907	0.9983	6.3553	2.5643
TSSE	1.3513	1.3355	0.0643	0.0770	0.8460	0.9752
RMSE	1.1624	1.1556	0.2537	0.2775	3.3683	0.5419
R^2	0.99991	0.99987	0.999934	0.99997	1.8353	0.7361
					0.8855	0.9784

Table 3. Efficiency values of T_{roof} model.

Modeling structure	ANFIS		Polynomial		Dynamic Model	Identification system
	Train data	Test data	Train data	Test data		
MAPE	5.3639	4.4446	0.8933	0.8770	8.0991	3.1946
EF	0.8909	0.9797	0.9969	0.9992	0.7996	0.9365
TSSE	0.8315	0.8902	0.0230	0.0323	6.7062	2.1234
RMSE	0.9118	0.9811	0.1518	0.1798	2.5896	1.4572
R^2	0.99996	0.99984	0.999997	0.999996	0.8944	0.9441

**Figure 3.** (a) Simulation results due to dynamical model and experimental data, and (b) Error responses.

assumptions are necessary to simplify these equations. Otherwise, measuring some coefficients will cost significantly. Therefore, with these simplifications, dynamic equations cannot be used to predict the greenhouse climate in a practical way. Therefore, models such as ANFIS and PNN can be simply implemented by using machine learning methods. They have lower coefficients than other methods such as multilayer neural networks and can be trained faster in industrial applications. It should be noted that, in this case, the only limitation of using these algorithms is to keep constant the variables that affect the physics of the problem

but are not involved in modelling. Otherwise, the model coefficients must be trained and updated at different predefined times.

Development of Greenhouse Climate Modeling with ANFIS and PNN

The modelling performed by Hongkang *et al.* (2018) by using the neural network method used 80% of the data for training and increased the modelling accuracy for T_{air} to $R^2 = 0.914$, $MAPE = 0.842$ and $RMSE = 1.504$. In other studies, on neural networks, to predict

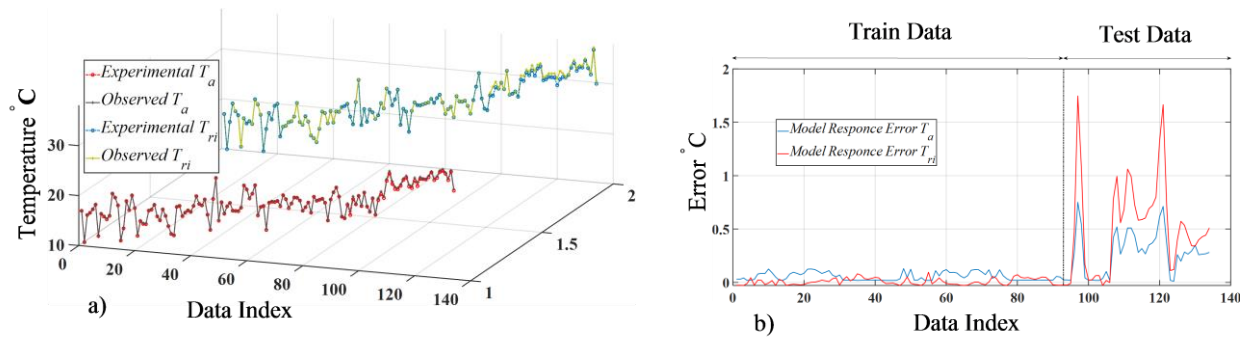


Figure 4. (a) Simulation results due to ANFIS model and experimental data, and (b) Error responses.

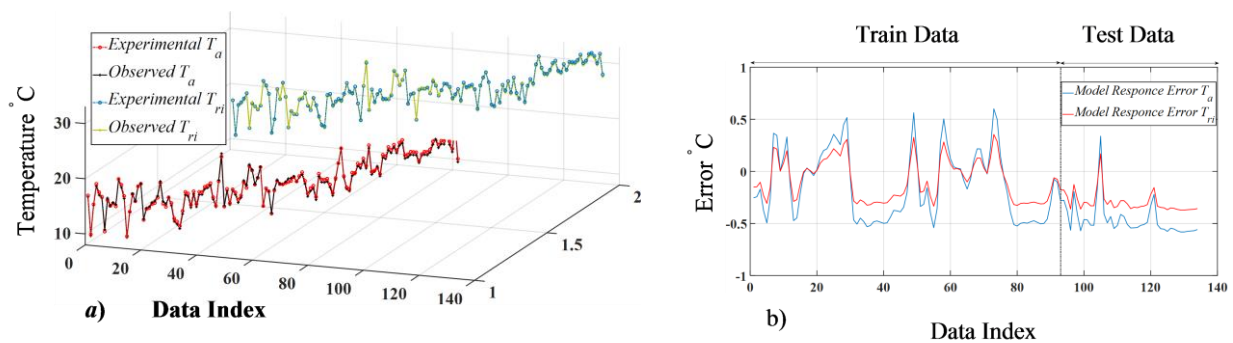


Figure 5. (a) Simulation results due to PNN model and experimental data, and (b) Error responses.

greenhouse temperatures, the *RMSE* was 0.94 and 0.9412, respectively for T_{air} (Jung *et al.*, 2020; Miranda and Castaño, 2017). Compared to Tables 2 and 3, the results show that ANFIS and PNN algorithms have higher accuracy than the neural network model. Furthermore, it should be noted that we used only 70% of the data set for training. Moreover, we used three and one layer of neurons in, respectively, ANFIS and PNN models. Therefore, the number of constant variables was lower, and the convergence rate of the model was higher than the neural network, which used more than 35 neurons in 3 hidden layers. As a result, the training speed in the proposed models was higher than neural networks.

The artificial intelligence algorithm can provide accurate predictions of parameters when there are no significant changes in the data pattern. In other words, when using the trained algorithm, the pattern of climate outside the greenhouse or the rate of evapotranspiration inside the greenhouse

should not change much compared to the time of data collection. In this case, the mentioned algorithms can be well used to predict and manage the climate inside the greenhouse or in the relevant climate control systems. In intelligent algorithms, type and data diversity will play an important role in application quality. At the time of data collection, the model can be made more practical by considering a greater variety of data that are more effective in greenhouse climate. In general, despite disturbances, uncertainties, and perturbations, the modelling response cannot be expected to be reliable in all circumstances. Therefore, the use of online identification algorithms along with modelling can provide a measure of system performance accuracy. The results of the identification algorithm used in this research are presented in the next section. It can be seen how this algorithm can be successful in confirming the greenhouse modelling response.

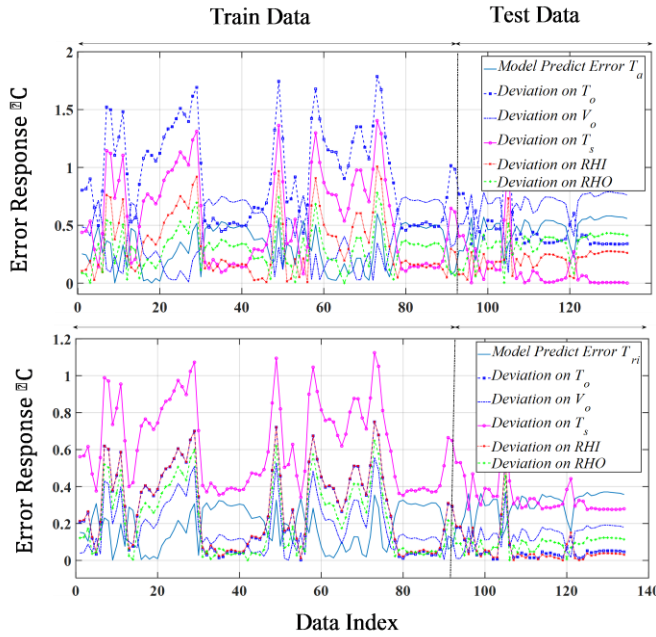


Figure 6. Sensitivity analysis due to deviation of +0.1.

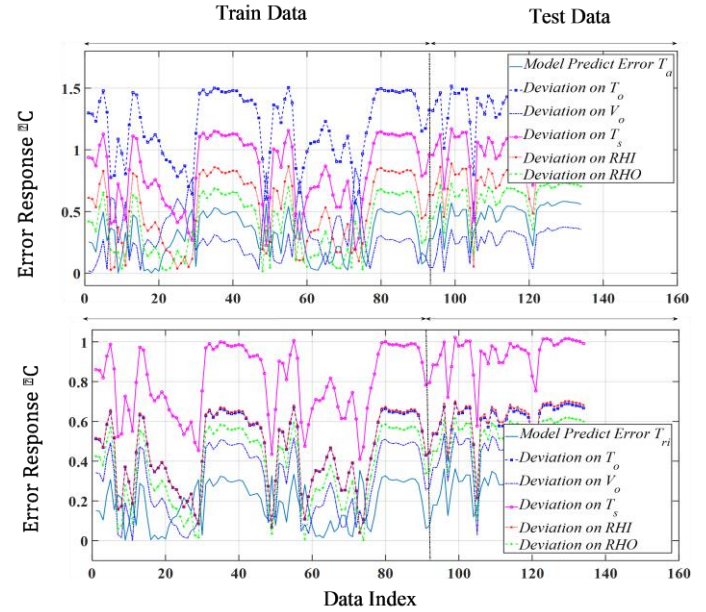


Figure 7. Sensitivity analysis due to deviation of -0.1.

Results of Greenhouse Temperature Identification

The proposed system identification Equation (24) was employed to identify the temperatures of T_{soil} , T_{air} and T_{roof} . Figure 9a shows the response of identification system with the use of sign function as To *et al.* (2009). The response of identification with sign function was much noisier than the response of system identification that was presented by Equation (24). Moreover, to achieve the performance of the identification procedure, the wavelet transform can be applied to denoise the data before use of Equation (24). The response of this procedure is depicted in Figure 9b, where the output of algorithm has converged to the experimental data. This method can be used on-line to identify the required states such as temperature and humidity everywhere in a greenhouse. Figure 9c shows that the proposed identification algorithm was converged after 5 sample times for T_{soil} and less than 2 sample times for T_{air} and T_{roof} . Therefore, it can be applied as an on-line estimator to predict all requirement states in a greenhouse or in the other industrial applications. The statistical results of the identification system for T_{soil} were presented

as follows: $MAPE = 2.05112$, $EF = 0.98928$, $TSSE = 0.22515$, $RMSE = 0.4745$, and $R^2 = 0.9949$. Moreover, the results of statistical calculations using identification system for prediction of $T_{air} = 17^\circ\text{C}$, and $T_{roof} = 17^\circ\text{C}$ are in Tables 2 and 3.

Comparing Figures 4, 5 and 9, we see that the results of modelling and online system identification were close to each other, and the results can be used with confidence. Since the mentioned identification method uses the results of differential equations online, the way it works is different from numerical modeling and artificial intelligence algorithms. Therefore, by comparing the model responses and identification, the system performance can be ensured. If there is a difference between the results, the system can be reset or a warning message or stop command can be sent to the operators and the user.

Depending on the application, modeling operations can deal with different types of data and sampling times. Since reducing the sampling time increases the sensitivity and increasing it reduces the accuracy, the choice of this sampling time will be different depending on the use. Moreover, one can never be sure that the

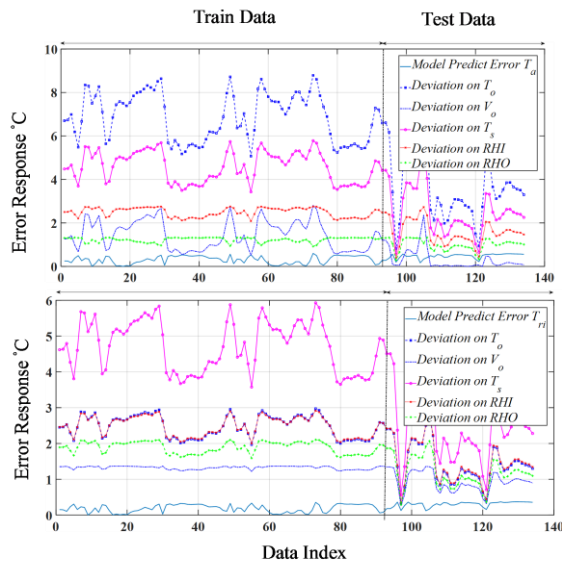


Figure 8. Sensitivity analysis due to removed inputs.

boundary conditions at the time of modeling exist is the same as the time of operation. Therefore, based on this study, to apply mathematical models industrially, it is suggested that several models should be used simultaneously with different identification algorithms and sampling time. It is also suggested that off-line modeling can be used to predict parameters whose sampling time is daily and longer. Additionally, on-line methods and identification algorithms can be used to predict the parameters to be measured at shorter sample times.

It should be noted that machine learning methods can predict any repetitive pattern with varying accuracy. In modelling, if we use many effective variables on the target, the accuracy of the model and the modeling challenge increases. This is more evident in the physical modelling of the system. To obtain a more complete dynamic model of the greenhouse, the Penman-Monteith Equation can be used to calculate the rate of evapotranspiration from meteorological. However, obtaining the parameters of these equations and measuring them will be costly and time consuming, which is beyond the scope of this study. However, it should be considered that sub-reactions and sub-dynamics are always present, and, therefore, their effect will be present in the data measured by the sensors. The

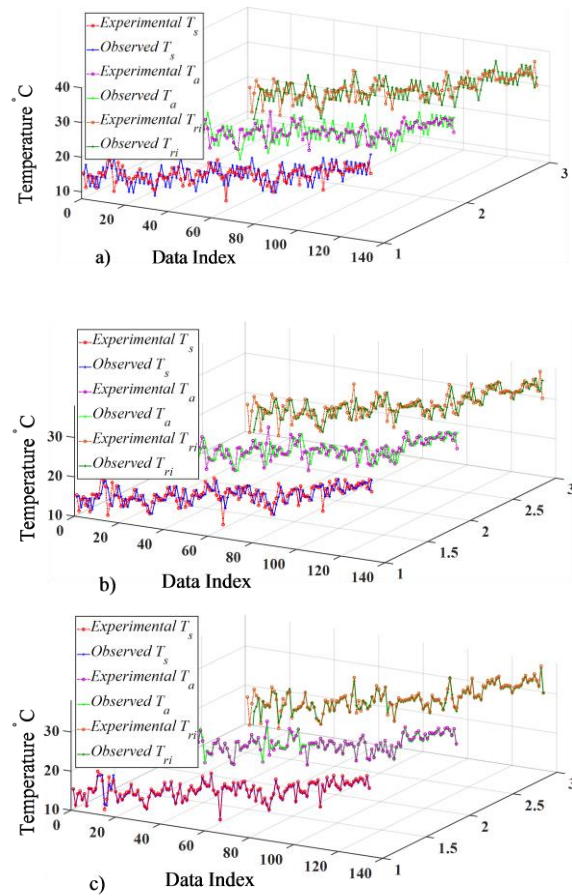


Figure 9. Identification responses as the results of (a) Sign function, (b) Smooth function, (c) Smooth function and wavelet transform.

trained model can be used independently to predict the desired parameters such as temperature, air, humidity, condensate, evapotranspiration as well as other greenhouse parameters. In this case, there will be an advantage that, without the use of direct data, the effect of all sub-reactions and sub-dynamics is easily considered.

CONCLUSIONS

In this study, a set of differential equation was derived as a dynamical model to find the temperature of inside air, inside roof cover, and topsoil for the constructed arch greenhouse. Moreover, a ANFIS mechanism and a PNN structure were proposed to predict and model the T_{air} and T_{roof} based on T_{out} , wind speed, T_{soil} ,



RH_{air} and RH_{out} . The SD-QPSO algorithm as a metaheuristic optimization algorithm was successfully applied to train the constant parameters of ANFIS and PNN structures.

The results showed that the proposed models were more accurate in predicting greenhouse climate and could be used more easily. Moreover, this study showed that the PNN model with less pop-size and evaluation function was more effective than the ANFIS structure to predict the temperatures of inside air and inside roof cover. We showed that by teaching the proposed models with only 70% of the data, their accuracy was higher than other similar references. Statistical analysis showed that R^2 and $RMSE$ increased by more than 0.08 and 0.34%, respectively. The sensitivity analysis was successfully performed by two different strategies. The results confirmed that the T_{out} , T_{soil} , RH_{air} , and RH_{out} were more effective on the T_{air} and T_{soil} . Moreover, T_{out} , RH_{air} and RH_{out} were also effective on the T_{roof} . An accurate dynamical model is hard to derive and needs much time for computation. Therefore, the proposed ANFIS and PNN structures with the SD-QPSO algorithm can be applied to nonlinear model and complicated physical behavior and its relations. Also, an identification system was proposed for real time prediction purposes and was successfully used to predict the T_{soil} , T_{air} and T_{roof} . It was shown that the use of wavelet transforms and substituting the sign function by the proposed function can improve the performance of the identification operation. The results showed that the online identification system could increase the prediction of T_{air} and T_{roof} by, respectively, 2.47 and 2.53 times in R^2 compared to the dynamic model. This accuracy showed that the identification system can be used for confirmation of the model and increasing the reliability of predicting operations. Therefore, this advantage can be used in greenhouse climate controllers.

Nomenclature

A_{soil} , A_{roof} and A_{nw} Soil, roof, and north wall surface area (m^2)

V_s , V_a and V_r The volume of Soil, inside air and roof (m^3)

ρ_s , ρ_a and ρ_r Density of soil, inside air, roof cover (kg/m^3)

c_{ps} , c_{pa} and c_{pr} Specific heat capacity ($J/kg K$) of soil, air and roof

λ_s and λ_{nw} Soil and north wall thermal conductivity ($W/m K$)

E_s , E_{ri} and E_{sk} Emission coefficient of soil, roof and sky

T_{soil} , T_{air} , and T_{roof} Temperature of Soil, inside air and roof (m^3)

T_{out} Temperature of the outside (K)

$\alpha_{a,s}$ Heat transfer coefficient, inside air to soil ($W/m^2 K$)

α_{rio} Heat transfer coefficient, inside roof to outside ($W/m^2 K$)

Q_{rds} Heat transfer, radiation absorption by soil (W)

Q_{sri} Heat transfer, soil to inside roof (W)

RH_{air} Inside air humidity

T_{ss} Temperature of the lower soil (K)

V_{out} Out wind speed (m/s)

ds and d_{nw} Upper soil and north wall Thickness (m)

T_{nwo} , T_{nwi} North wall out and in temperature (K)

f_a Infiltration Factor

F_{sri} , F_{risk} Soil-roof and roof-sky View factor

η_{sis} Absorption coefficient of shortwave radiation by soil

η_{roofIs} Absorption coefficient shortwave radiation by roof

I_{roof} Solar radiation, inside roof (W/m^2)

I_{in} Solar radiation, upper soil (W/m^2)

Q_{risk} Heat transfer, inside roof to sky (W)

Q_{rdri} Heat transfer, radiation absorption by roofs (W)

RH_{out} Outside air humidity

REFERENCES

- Chen, J., Yang, J., Zhao, J., Xu, F., Shen, Z. and Zhang, L. 2016. Energy Demand Freccasting of the Greenhouses Using Nonlinear Models Based on Model Optimized Prediction Method. *Neurocomputing*, **174(Part B)**:1087-1100.

2. De-Zwart, H. F. 1996. Analyzing Energy-Saving Options in Greenhouse Cultivation Using a Simulation Model. PhD Dissertation, Agricultural University, Wageningen, The Netherlands, 236 PP.
3. Ferreira, P. M., Faria, E. A. and Ruano, A. E. 2002. Neural Network Models in Greenhouse Air Temperature Prediction. *Neurocomputing*, **43**: 51–75.
4. Fidaros, D. K., Baxevanou, C. A., Bartzanas, T. and Kittas, C. 2010. Numerical Simulation of Thermal Behavior of a Ventilated Arc Greenhouse during a Solar Day. *Renew. Energy*, **35**: 1380–1386.
5. Floquet, T. and Barbot, J. P. 2007. Super Twisting Algorithm-Based Step-by-Step Sliding Mode Observers for Nonlinear Systems with Unknown Inputs. *Int. J. Syst. Sci.*, **38**(10):803–815.
6. Fourati, F. and Chtourou, M. 2007. A Greenhouse Control with Feed-Forward and Recurrent Neural Networks. *Simul. Model. Pract. Theory*. **15**:1016–1028.
7. Fridman, L., Levant, A. and Davila, J. 2007. Observation of Linear Systems with Unknown Inputs via High-Order Sliding-Modes. *Int. J. Syst. Sci.*, **38**(10): 773–791.
8. García, A. E., Zarazúa, G. M. S., Ayala, M. T., Araiza, E. R. and Barrios, A. G. 2020. Applications of Artificial Neural Networks in Greenhouse Technology and Overview for Smart Agriculture Development. *Appl. Sci.*, **10**: 3835.
9. Grigoriu, R. O., Voda, A., Arghira, N. and Iliescu, S. S. 2015. Modelling of Greenhouse using Parabolic Trough Collectors Thermal Energy. *IFAC-Papers OnLine*, **48**(30): 450–455.
10. González, I. and Calderón, A. J. 2018. Neural Networks-Based Models for Greenhouse Climate Control. *The XXXIX Automatic Conference*, September 5-7, Badajoz, Spain.
11. He, F. and Ma, C. 2010. Modeling Greenhouse Air Humidity by Means of Artificial Neural Network and Principal Component Analysis. *Comput. Electron. Agric.*, **71**: 19–23.
12. Hongkang, W. Li, L., Yong, W., Fanjia, M., Haihua, W. and Sigrimis, N. A. 2018. Recurrent Neural Network Model for Prediction of Microclimate in Solar Greenhouse. *IFAC Papers OnLine*, **51**(17): 790-795.
13. Hu, H., Xu, L., Goodman, E. D. and Zeng, S. 2014. NSGA-II-Based Nonlinear PID Controller Tuning of Greenhouse Climate for Reducing Costs and Improving Performances. *Neural Comput. Appl.*, **24**(3-4): 927-936.
14. Isaev, S. M. and Sadykov, Z. D. 2014. A Mathematical Model of Heat Exchange Control in Solar Greenhouses. *Appl. Solar Energy*, **50**(2):103–109.
15. Jang, J. S. R. 1993. ANFIS: Adaptive-Network-Based Fuzzy Inference System. *IEEE Trans. Syst. Man Cybern. Syst.*, **23**(3).
16. Joudi, K. and Farhan, A. 2007. A Dynamic Model and an Experimental Study for the Internal Air and Soil Temperatures in an Innovative Greenhouse. *Energy Convers. Manage.*, **91**: 76–82.
17. Jung, D. H., Kim, H. S., Jhin, C., Kim, H. J. and Park, S. H. 2020. Time-Serial Analysis of Deep Neural Network Models for Prediction of Climatic Conditions inside a Greenhouse. *Comput. Electron. Agric.*, **173**: 105402.
18. Kurtulus, B., Flipo, N. and Goblet, P. 2010. Sensitivity Analysis on an Adaptive Neuro Fuzzy Inference System (ANFIS) for Hydraulic Head Interpolation: Orgeval Experimental SITE/France. In: “XVIII International Conference on Water Resources CMWR 2010”, (Ed.): Carrera, J. ©CIMNE, Barcelona.
19. Levant, A. 1993. Sliding Order and Sliding Accuracy in Sliding Mode Control. *Int. J. Control*, **58**(6): 1247–1263.
20. Márquez-Vera, M. A., Ramos-Fernández, J. C. and Cerecero-Natale, L. F. 2016. Temperature Control in a MISO Greenhouse by Inverting its Fuzzy Model. *Comput. Electron. Agric.*, **124**: 168–174.
21. Miranda, A. C. and Castaño, V. M. 2017. Smart Frost Control in Greenhouses by Neural Networks Models. *Comput. Electron. Agric.*, **137**: 102-114.
22. Mobtaker, H. G., Ajabshirchi, Y., Ranjbar, S. F. and Matloobi, M. 2016. Solar Energy



- Conservation in Greenhouse: Thermal Analysis and Experimental Validation. *Renew. Energy*, **96**: 509-519.
23. Moghaddam, J. J. and Bagheri, A. 2015. A Novel Stable Deviation Quantum-Behaved Particle Swarm Optimization to Optimal Piezoelectric Actuator and Sensor Location for Active Vibration Control. *Proc. Inst. Mech. Eng. Pt. I: J. Syst. Contr. Eng.*, **229(6)**: 485-494.
24. Pasgianos, G. D., Arvanitis, K. G., Polycarpou, P. and Sigrimis, N. 2003. A Nonlinear Feedback Technique for Greenhouse Environmental Control. *Comput. Electron. Agric.*, **40**: 153-177.
25. Patila, S. L., Tantaua, H. J. and Salokheeb, V. M. 2008. Modelling of Tropical Greenhouse Temperature by Auto Regressive and Neural Network Models. *Biosyst. Eng.*, **99**: 423-431.
26. Perez-Gonzalez, A., Begovich-Mendoza, O. and Ruiz-Leon, J. 2017. Modeling of a Greenhouse Prototype Using PSO and Differential Evolution Algorithms Based on a Real-Time LabView™ Application. *Appl. Soft Comput.*, **62**: 86 – 100.
27. Rosas, A. R., Molina-Aiz, F. D., Valera, D. L., López, A. and Khamkure, S. 2017. Development of a Single Energy Balance Model for Prediction of Temperatures inside a Naturally Ventilated Greenhouse with Polypropylene Soil Mulch. *Comput. Electron. Agric.*, **142**: 9–28.
28. Sethi, V. P., Sumathy, K., Lee, C. and Pal, D. S. 2013. Thermal Modeling Aspects of Solar Greenhouse Microclimate Control: A Review on Heating Technologies. *Solar Energy*, **96**: 56–82.
29. Speetjens, S. L., Stigter, J. D. and Straten, G. V. 2009. Towards an Adaptive Model for Greenhouse Control. *Comput. Electron. Agric.*, **67**: 1–8.
30. Su, Y. and Xu, L. 2017. Towards Discrete Time Model for Greenhouse Climate Control. *Eng. Agric. Environ. Food*, **10(2)**: 157-170.
31. Su, Y., Xu, L. and Li, D. 2016. Adaptive Fuzzy Control of a Class of MIMO Nonlinear System with Actuator Saturation for Greenhouse Climate Control Problem. *IEEE Trans. Autom. Sci. Eng.*, **13(2)**: 772 - 788.
32. Taki, M., Ajabshirchi, Y., Ranjbar, S. F., Rohani, A. and Matloobi, M. 2016. Heat Transfer and MLP Neural Network Models to Predict Inside Environment Variables and Energy Lost in a Semi-Solar Greenhouse. *Energy Build.*, **110**: 314-329.
33. To, A. C., Moore, J. R. and Glaser, S. D. 2009. Wavelet Denoising Techniques with Applications to Experimental Geophysical Data. *Signal Proces.*, **89(2)**: 144-160.
34. Vadiiee, A. 2011. Energy Analysis of the Closed Greenhouse Concept-Toward one Sustainable Energy Pathway. Division of Heat and Power Technology, KTH School of Industrial Engineering and Management, Department of Energy Technology, SE-100 44 Stockholm.
35. Van-Ooteghem, R. J. C. 2007. Optimal Control Design for a Solar Greenhouse, Systems and Control. Wageningen University, The Netherlands.
36. Van-Straten, G., Van-Willigenburg, G., Van-Henten, E. and Van-Ootghem, R. 2011. Optimal Control of 682 Greenhouse Cultivation. CRC press, Taylor and Francis, New York.
37. Yau, H. T. and Chen, C. L. 2011. Fuzzy Sliding Mode Controller Design for Maximum Power Point Tracking Control of a Solar Energy System. *Trans. Inst. Meas. Control*, **34(5)**: 557–565.
38. Yu, H., Chen, Y., Gul Hassan, S. and Li, D. 2016. Prediction of the Temperature in a Chinese Solar Greenhouse Based on LSSVM Optimized by Improved PSO. *Comput. Electron. Agric.*, **122**: 94–102.
39. Ziapour, B. M. and Dehnavi, R. 2012. A Numerical Study of the Arc-Roof and the One-Sided Roof Enclosures Based on the Entropy Generation Minimization. *Comput. Math. Appl.*, **64**: 1636–1648.

مدل‌های حرارتی، ANFIS و یک شبکه عصبی چند جمله‌ای برای پیش‌بینی متغیرهای اقلیمی یک گلخانه کمانی

ج. جوادی مقدم، د. مومنی، و ق. زارعی

چکیده

هدف از این مطالعه طراحی یک مکانیسم استنتاج عصبی فازی تطبیقی (ANFIS) و یک شبکه عصبی چند جمله‌ای (PNN) برای بهبود مدل‌سازی و شناسایی برخی متغیرهای آب و هوایی در یک گلخانه است. علاوه بر این، یک الگوریتم بهینه‌سازی ازدحام ذرات با رفتار کوانتومی پایدار (SD-QPSO) به عنوان یک الگوریتم یادگیری برای آموزش پارامترهای ثابت ساختارهای ANFIS و PNN استفاده شد. برای حذف نویز داده‌های اندازه‌گیری شده، از روش تبدیل موجک استفاده می‌شود تا اطمینان حاصل شود که هیچ داده اندازه‌گیری شده از یک بازه از پیش تعریف شده فراتر نمی‌رود. علاوه بر این، برای نشان دادن عملکرد مدل‌سازی، مجموعه‌ای از معادلات دیفرانسیل به عنوان یک مدل دینامیکی بر اساس رابطه انرژی و تعادل جرم در یک گلخانه مشخص به دست آمدند. برای اهداف شبیه‌سازی، دمای سطح خاک، هوای داخلی و پوشش سقف گلخانه برای مدل ANFIS، PNN و دینامیکی در نظر گرفته شد. نتایج مدل‌سازی و شبیه‌سازی با نتایج تجربی یک گلخانه آزمایشی کمانی ارزیابی شد. نتایج نشان داد که مدل‌های پیشنهادی در پیش‌بینی اقلیم گلخانه دقیق‌تر بوده و به راحتی قابل استفاده هستند. علاوه بر این، این مطالعه نشان داد که مدل PNN با اندازه جمعیت کمتر از ساختار ANFIS برای پیش‌بینی دمای هوای داخل و سقف مؤثرتر بود. در این مطالعه، یک سیستم شناسایی آنلاین نیز برای شناسایی بلادرنگ داده‌های تجربی پیشنهاد شد. نتایج شبیه‌سازی به دست آمده نشان داد که عملکرد مدل پیشنهادی و سیستم شناسایی برای پیش‌بینی و شناسایی دمای سطح خاک، هوای داخلی و پوشش سقف گلخانه مؤثر بود. این مطالعه نشان داد که الگوریتم شناسایی می‌تواند برای پیش‌بینی و تایید نتایج مدل استفاده شود. در نهایت، نتایج تحلیل حساسیت روی مدل‌ها نشان داد که دمای داخل و سقف گلخانه چگونه توانست تحت تأثیر دمای بیرون و خاک قرار بگیرد.